# Comparison of DTR spectral-angular characteristics of divergent beam of relativistic electrons in scattering geometry of Laue and Bragg



# Comparison of DTR spectral-angular characteristics of divergent beam of relativistic electrons in scattering geometry of Laue and Bragg

**S V Blazhevich, T V Koskova, A Z Ligidov, A V Noskov**
Belgorod State University, Belgorod, Russia

E-mail: noskovbupk@mail.ru

**Abstract.** Diffracted transition radiation (DTR) generated by a divergent beam of relativistic electrons crossing a single-crystal plate in different (Laue, Bragg) scattering geometry has been considered for the general case of asymmetric reflection of the electron coulomb field relative to the entrance target surface. The expressions for spectral-angular density of DTR and parametric X-ray Radiation (PXR) has been derived. Then DTR and PXR has been considered in case of a thin target, when multiple scattering of electron is negligibly small, which is important for divergence measurement in real time regime. Numerical calculation of spectral-angular density of DTR by a beam of relativistic electrons has been made using averaging over the bivariate Gauss distribution as angular distribution of relativistic electrons in the beam. It has been shown that in Bragg scattering geometry the angular density of DTR is bigger, than in Laue geometry, which can be explained by the existence of the frequency range, in which the incident wave propagation vector takes complex value even under absence of absorption. In this range, all of photons are reflected in Bragg direction. It means that the range of total reflection defines the width of DTR spectrum.

## 1. Introduction

In the physics of interaction of relativistic electrons with matter, is important for the experimental data interpretation to know spatial and angular distributions of particles in the incident beam. That is why working out express methods of obtaining information about the characteristics of the beam used in the experiment is actual problem. One of the approaches is to use different types of radiation excited by relativistic charged particles in matter. Recently the possibility of use of parametric X-radiation (PXR) for the diagnostics of relativistic electron beams was experimentally studied in [1, 2]. In [3] it was suggested using PXR generated in a thin crystal to get operative information on spatial distribution of the relativistic electron beam. The applicability of transition radiation (TR) of vacuum ultraviolet range to measure the electron beam cross dimensions was demonstrated in [4]. The authors of [5] suggest the use of X-ray Cherenkov radiation by ultrarelativistic charged particles in the photon energy range, which includes K-absorption edges for some of the materials, to reveal the cross-dimensions of the beam.

In all the above-listed works, the beam parameters estimation was carried out in the framework of kinematic PXR theory, therefore studying the influence of dynamic effects on the characteristics of coherent radiation by relativistic electron beams remains an important task.

As we know PXR appears due to the scattering of a relativistic electron Coulomb field on a system of parallel atomic planes in the crystal [6–8]. When a charged particle crosses the crystal plate surface, the transition radiation (TR) takes place [9, 10]. TR appearing on the border diffracts then on a system of parallel atomic planes of the crystal which forms DTR in a narrow spectral range [11–14]. The DTR photons move near the Bragg scattering direction.

The process of coherent X-ray radiation by a single relativistic electron in a crystal is described in the framework of the dynamical theory of x-rays diffraction in [15–18]. In these papers, the dynamic theory of coherent X-ray radiation generated by a relativistic electron in a crystal are built for general case of asymmetric relative to the crystal (target) surface reflection of the electron Coulomb field. In this case, the system of the parallel reflecting atomic planes in the target can be located at arbitrarily given angle to the target surface. Under these conditions, coherent X-radiation in the direction of the Bragg scattering appears because of two coherent radiation mechanisms, namely PXR and DTR.
In the present work, a dynamical theory of coherent X-ray radiation generated in a single-crystal target by a divergent beam of relativistic electrons has been developed both in Laue and Bragg scattering geometries.

## 2. Radiation process geometries

Let us consider a beam of relativistic electrons crossing a monocrystalline plate in of Laue (figure 1) and Bragg (figure 2) scattering geometries.

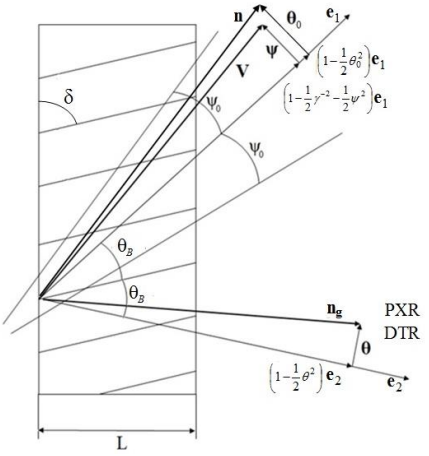


**Figure 1.** Laue scattering geometry.

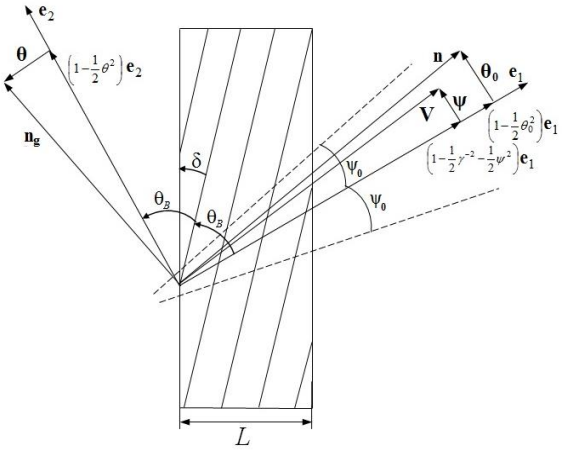


**Figure 2.** Bragg scattering geometry.

Let us involve the angular variables $\boldsymbol{\psi}$, $\boldsymbol{\theta}$ and $\boldsymbol{\theta}_0$ in accordance with the definition of relativistic electron velocity $\mathbf{V}$ and unit vectors in direction of momentum of the photon radiated in the direction near electron velocity vector $\mathbf{n}$ and in the Bragg scattering direction $\mathbf{n}_\mathbf{g}$:

$$\mathbf{V}=\left(1-\frac{1}{2}\gamma^{-2}-\frac{1}{2}\psi^2\right)\mathbf{e}_1+\boldsymbol{\psi},\ \mathbf{e}_1\boldsymbol{\psi}=0,\ \mathbf{n}=\left(1-\frac{1}{2}\theta_0^2\right)\mathbf{e}_1+\boldsymbol{\theta}_0,\quad \mathbf{e}_1\boldsymbol{\theta}_0=0,\quad \mathbf{e}_1\mathbf{e}_2=\cos 2\theta_B$$

$$\mathbf{n}_\mathbf{g}=\left(1-\frac{1}{2}\theta^2\right)\mathbf{e}_2+\boldsymbol{\theta},\ \mathbf{e}_2\boldsymbol{\theta}=0, \tag{1}$$

where $\boldsymbol{\theta}$ is the radiation angle, counted from direction of axis of radiation detector $\mathbf{e}_2$, $\boldsymbol{\psi}$ is the incidence angle of an electron in the beam counted from the electron beam axis $\mathbf{e}_1$, $\boldsymbol{\theta}_0$ is the angle between the movement direction of incident photon and axis $\mathbf{e}_1$, $\gamma=1/\sqrt{1-V^2}$ is Lorentz-factor of the particle. The angular variables are decomposed into the components parallel and perpendicular to

the figure plane: $\boldsymbol{\theta}=\boldsymbol{\theta}_{||}+\boldsymbol{\theta}_{\perp}$, $\boldsymbol{\theta}_0=\boldsymbol{\theta}_{0||}+\boldsymbol{\theta}_{0\perp}$, $\boldsymbol{\psi}=\boldsymbol{\psi}_{||}+\boldsymbol{\psi}_{\perp}$, $\psi_0$ is the divergence parameter of the beam of radiating electrons.

Let us consider the electromagnetic processes in the crystalline medium characterized by the complex permittivity

$$\varepsilon(\omega,\mathbf{r})=1+\chi(\omega,\mathbf{r}), \tag{2}$$

where $\chi(\omega,\mathbf{r})=\chi_0(\omega)+\sum_{\mathbf{g}}\chi_{\mathbf{g}}(\omega)\exp(i\mathbf{g}\mathbf{r})$, $\chi(\omega,\mathbf{r})$ is the dielectric susceptibility, $\chi_{\mathbf{g}}(\omega)=\chi'_{\mathbf{g}}(\omega)+i\chi''_{\mathbf{g}}(\omega)$ is the Fourier coefficient of the expansion of the dielectric susceptibility of the crystal in reciprocal lattice vectors $\mathbf{g}$, and $\chi_0(\omega)$ is the average dielectric susceptibility.

In this work the two-wave approach of dynamic diffraction theory are used, in which both the incident and diffracted waves are considered as equitable in process of self-repumping one into another in crystalline target. While solving the problem, let us consider an equation for a Fourier image of an electromagnetic field $\mathbf{E}(\mathbf{k},\omega)=\int dt\,d^3\mathbf{r}\,\mathbf{E}(\mathbf{r},t)\exp\left(i\omega t-i\mathbf{k}\mathbf{r}\right)$. The strengths of electromagnetic fields, excited by electron in the crystal are

$$\begin{aligned}\mathbf{E}(k,\omega)&=E_0^{(1)}(\mathbf{k},\omega)\mathbf{e}_0^{(1)}+E_0^{(2)}(\mathbf{k},\omega)\mathbf{e}_0^{(2)},\\ \mathbf{E}(\mathbf{k}+\mathbf{g},\omega)&=E_{\mathbf{g}}^{(1)}(\mathbf{k},\omega)\mathbf{e}_1^{(1)}+E_{\mathbf{g}}^{(2)}(\mathbf{k},\omega)\mathbf{e}_1^{(2)},\end{aligned} \tag{3}$$

$\mathbf{e}_0^{(1)}\perp\mathbf{k}$, $\mathbf{e}_0^{(2)}\perp\mathbf{k}$, $\mathbf{e}_1^{(1)}\perp\mathbf{k}_{\mathbf{g}}$ и $\mathbf{e}_1^{(2)}\perp\mathbf{k}_{\mathbf{g}}$, $\mathbf{k}_{\mathbf{g}}=\mathbf{k}+\mathbf{g}$. Vectors $\mathbf{e}_0^{(2)}$, $\mathbf{e}_1^{(2)}$ are situated on the plane of vectors $\mathbf{k}$ и $\mathbf{k}_{\mathbf{g}}$ ($\pi$-polarization) and $\mathbf{e}_0^{(1)}$, $\mathbf{e}_1^{(1)}$ are perpendicular to this plane ($\sigma$-polarization);

The system of equations for the Fourier transform images of the electromagnetic field in a two wave approximation of dynamic theory of diffraction has the following form [19].

For the Laue scattering geometry the system of equations has a view

$$\begin{cases}(\omega^2(1+\chi_0)-k^2)E_0^{(s)}+\omega^2\chi_{-\mathbf{g}}C^{(s)}E_{\mathbf{g}}^{(s)}=8\pi^2ie\omega\mathbf{e}_0^{(s)}\mathbf{V}\delta(\omega-\mathbf{k}\mathbf{V}),\\ \omega^2\chi_{\mathbf{g}}C^{(s)}E_0^{(s)}+(\omega^2(1+\chi_0)-k_{\mathbf{g}}^2)E_{\mathbf{g}}^{(s)}=0,\end{cases} \tag{4}$$

where $C^{(s)}=\mathbf{e}_0^{(s)}\mathbf{e}_1^{(s)}$, $C^{(1)}=1$, $C^{(2)}=\cos2\theta_B$.Equations set (4) under $s=1$ describes the fields of $\sigma$-polarization, and under s = 2 the fields of $\pi$-polarization.

For the Bragg scattering geometry the system of equations has a view

$$\begin{cases}(\omega^2(1+\chi_0)-k^2)E_0^{(s)}+\omega^2\chi_{-\mathbf{g}}C^{(s,\tau)}E_{\mathbf{g}}^{(s)}=8\pi^2ie\omega\mathbf{e}_0^{(s)}\mathbf{V}\delta(\omega-\mathbf{k}\mathbf{V}),\\ \omega^2\chi_{\mathbf{g}}C^{(s,\tau)}E_0^{(s)}+(\omega^2(1+\chi_0)-k_{\mathbf{g}}^2)E_{\mathbf{g}}^{(s)}=0,\end{cases} \tag{5}$$

where $C^{(s,\tau)}=\mathbf{e}_0^{(s)}\mathbf{e}_1^{(s)}=(-1)^{\tau}C^{(s)}$, $C^{(1)}=1$, $C^{(2)}=\left|\cos2\theta_B\right|$.

The system of equations (5) for $s=1$ and $\tau=2$ describes the $\sigma$-polarized fields. For $s=2$, the system of equations (5) describes $\pi$-polarized fields; note that if $2\theta_B<\frac{\pi}{2}$, then $\tau=2$, otherwise $\tau=1$. In the system of equations (4) и (5) following table of symbols is denoted

$$\begin{aligned}&P^{(1)}=\sin\varphi,\ P^{(2)}=\cos\varphi,\ \mathbf{e}_0^{(1)}\mathbf{V}=(\theta-\psi)P^{(1)}=\theta_{\perp}-\psi_{\perp},\ \mathbf{e}_0^{(2)}\mathbf{V}=(\theta+\psi)P^{(2)}=\theta_{//}+\psi_{//},\\ &\chi'_{\mathbf{g}}=\chi'_0(F(g)/Z)(S(\mathbf{g})/N_0)\exp\left(-g^2u_{\tau}^2/2\right),\ \chi''_{\mathbf{g}}=\chi''_0\exp\left(-\frac{1}{2}g^2u_{\tau}^2\right),\end{aligned} \tag{6}$$

where $\chi_0=\chi'_0+i\chi''_0$ – is the average dielectric susceptibility, F(g) – is the form factor of atom containing Z electrons, $S(\mathbf{g})$ is the structural factor of a unit cell containing $N_0$ atoms, $u_{\tau}$ is the r.m.s. amplitude of thermal vibrations of crystal atoms. The work addresses the X-ray frequency range, where $\chi'_{\mathbf{g}}<0,\chi'_0<0$. We will consider a crystal with the following symmetry ($\chi_g=\chi_{-g}$), $\varphi$ is the azimuthal radiation angle measured from the plane formed by the vectors $\mathbf{V}$ и $\mathbf{g}$, the value of the

reciprocal lattice vector is determined by the $g = 2\omega_B \sin\theta_B / V$, where $\omega_B$ is the Bragg frequency.

### 3. Spectral-angular density of PXR and DTR in a thin crystal

Let us consider the relativistic electron coherent X-radiation in Laue scattering geometry (see figure 1). If we perform the analytical procedures similar to those used in [20, 21] we will obtain the expressions for the spectral-angular density of PXR and DTR for the propagation direction of the emitted photon $\mathbf{k_g} = k_\mathbf{g}\mathbf{n_g}$ (see. figure 1) taking into account the direction deviation of the electron velocity $\mathbf{V}$ relative to the electron beam axis $\mathbf{e}_1$

$$\omega\frac{d^2N^{(s)}_{\mathrm{PXR}}}{d\omega d\Omega} = \frac{e^2}{\pi^2}\frac{\Omega^{(s)2}}{(\gamma^{-2}+(\theta_\perp-\psi_\perp)^2+(\theta_{//}+\psi_{//})^2-\chi_0')^2}R^{(s)}_{\mathrm{PXR}}, \tag{7a}$$

$$R^{(s)}_{\mathrm{PXR}} = \left(1-\frac{\xi^{(s)}}{\sqrt{\xi^{(s)2}+\varepsilon}}\right)^2\sin^2\left(\frac{b^{(s)}}{2}\left(\sigma^{(s)}+\frac{\xi^{(s)}-\sqrt{\xi^{(s)2}+\varepsilon}}{\varepsilon}\right)\right)\left(\sigma^{(s)}+\frac{\xi^{(s)}-\sqrt{\xi^{(s)2}+\varepsilon}}{\varepsilon}\right)^{-2}, \tag{7b}$$

$$\omega\frac{d^2N^{(s)}_{\mathrm{DTR}}}{d\omega d\Omega} = \frac{e^2}{\pi^2}\Omega^{(s)2}\left(\frac{1}{\gamma^{-2}+(\theta_\perp-\psi_\perp)^2+(\theta_{//}+\psi_{//})^2}-\frac{1}{\gamma^{-2}+(\theta_\perp-\psi_\perp)^2+(\theta_{//}+\psi_{//})^2-\chi_0'}\right)^2 R^{(s)}_{\mathrm{DTR}}, \tag{8a}$$

$$R^{(s)}_{DTR} = \frac{\varepsilon^2}{\xi^{(s)2}+\varepsilon}\sin^2\left(b^{(s)}\frac{\sqrt{\xi^{(s)2}+\varepsilon}}{\varepsilon}\right), \tag{8b}$$

where

$$\Omega^{(1)} = \theta_\perp-\psi_\perp,\ \Omega^{(2)} = \theta_{//}+\psi_{//}, \sigma^{(s)} = \frac{1}{\left|\chi_\mathbf{g}'\right|C^{(s)}}\left(\gamma^{-2}+(\theta_\perp-\psi_\perp)^2+(\theta_{//}+\psi_{//})^2-\chi_0'\right),$$

$$\varepsilon = \frac{\sin(\delta+\theta_B)}{\sin(\delta-\theta_B)},\ b^{(s)} = \frac{1}{2\sin(\delta-\theta_B)}\frac{L}{L^{(s)}_{ext}},\ \xi^{(s)}(\omega) = \eta^{(s)}(\omega)+\frac{1-\varepsilon}{2\nu^{(s)}},\ L^{(s)}_{ext} = 1/\omega\left|\chi_\mathbf{g}'\right|C^{(s)},$$

$$\eta^{(s)}(\omega) = \frac{2\sin^2\theta_B}{V^2\left|\chi_\mathbf{g}'\right|C^{(s)}}\left(1-\frac{\omega(1-\theta_{//}\cot\theta_B)}{\omega_B}\right),\ \nu^{(s)} = \frac{\chi_\mathbf{g}'C^{(s)}}{\chi_0'}. \tag{9}$$

The parameter $\varepsilon$ is an important parameter in (2) - (4); it determines the degree of asymmetry of the reflection of the field in a crystal plate with respect to the target surface. Note that the angle of electron incidence on the target surface $\delta-\theta_B$ increases when the $\varepsilon$ parameter decreases, and vice versa.

Parameter $b^{(s)}$ characterizing the thickness of the crystal plate is the ratio of half of the path of the electron in the target $L_e = L/\sin(\delta-\theta_B)$ to the extinction length $L^{(s)}_{ext}$. Parameter $\nu^{(s)}$ can take the values in the interval $0\le\nu^{(s)}\le1$ and determines the degree of reflection of the waves from the crystal, which is caused by the nature of the interference of the waves reflected from different planes (constructive ($\nu^{(s)}\approx1$) or destructive ($\nu^{(s)}\approx0$)). The spectral function $\eta^{(s)}(\omega)$ rapidly changes with the frequency of the radiation therefore this function is convenient for use as an argument in the diagrams demonstrating the spectra of PXR and DTR .

Let us consider the relativistic electron coherent X-radiation in Bragg scattering geometry (see figure 2). If we perform the analytical procedures similar to those used in [22] we will obtain the expressions for the spectral-angular density of PXR and DTR for the propagation direction of the emitted photon $\mathbf{k_g} = k_\mathbf{g}\mathbf{n_g}$ (see. figure 2) taking into account the direction deviation of the electron velocity $\mathbf{V}$ relative to the electron beam axis $\mathbf{e}_1$

$$\omega\frac{d^2N_{\mathrm{PXR}}^{(s)}}{d\omega d\Omega}=\frac{e^2}{\pi^2}\frac{\Omega^{(s)^2}}{\left(\gamma^{-2}+(\theta_\perp-\psi_\perp)^2+(\theta_{//}+\psi_{//})^2-\chi_0'\right)^2}R_{\mathrm{PXR}}^{(s)}, \tag{10a}$$

$$R_{\mathrm{PXR}}^{(s)}=\frac{\left(\xi^{(s)}+\sqrt{\xi^{(s)^2}-\varepsilon}\right)^2}{\xi^{(s)^2}-\varepsilon+\varepsilon\sin^2\left(\dfrac{b^{(s)}\sqrt{\xi^{(s)^2}-\varepsilon}}{\varepsilon}\right)}\frac{\sin^2\left(\dfrac{b^{(s)}}{2}\left(\dfrac{\xi^{(s)}+\sqrt{\xi^{(s)^2}-\varepsilon}}{\varepsilon}-\sigma^{(s)}\right)\right)}{\left(\dfrac{\xi^{(s)}+\sqrt{\xi^{(s)^2}-\varepsilon}}{\varepsilon}-\sigma^{(s)}\right)^2}, \tag{10b}$$

$$\omega\frac{d^2N_{\mathrm{DTR}}^{(s)}}{d\omega d\Omega}=\frac{e^2}{\pi^2}\Omega^{(s)^2}\left(\frac{1}{\gamma^{-2}+(\theta_\perp-\psi_\perp)^2+(\theta_{//}+\psi_{//})^2}-\frac{1}{\gamma^{-2}+(\theta_\perp-\psi_\perp)^2+(\theta_{//}+\psi_{//})^2-\chi_0'}\right)^2R_{\mathrm{DTR}}^{(s)}, \tag{11a}$$

$$R_{\mathrm{DTR}}^{(s)}=\frac{\varepsilon^2}{\xi^{(s)^2}-\left(\xi^{(s)^2}-\varepsilon\right)\coth^2\left(\dfrac{b^{(s)}\sqrt{\varepsilon-\xi^{(s)^2}}}{\varepsilon}\right)}, \tag{11b}$$

where the notations analogous to (4) are used:

$$C^{(2)}=\left|\cos 2\theta_B\right|,\ \varepsilon=\frac{\sin(\theta_B-\delta)}{\sin(\theta_B+\delta)},\ b^{(s)}=\frac{1}{2\sin(\theta_B+\delta)}\frac{L}{L_{ext}^{(s)}},\ \xi^{(s)}(\omega)=\eta^{(s)}(\omega)+\frac{1+\varepsilon}{2\nu^{(s)}}. \tag{12}$$

Under a fixed value of $\theta_B$ the value $\varepsilon$ defines the orientation of crystal plate in relation to the system of diffracting atomic planes. When the angle of electron incidence on the target surface $\theta_B+\delta$ decreases the value of $\delta$ parameter can become negative and then will increase in magnitude (in extreme case $\delta\to-\theta_B$) that leads to increase of $\varepsilon$. On the contrary, when the angle of electron incidence decreases the value of $\varepsilon$ decrease (in extreme case $\delta\to\theta_B$).

The expressions (7), (10) and (8), (11) describe the spectral-angular density of PXR and DTR of the relativistic electron crossing a crystal plate at an angle $\boldsymbol{\psi}(\psi_\perp,\psi_{//})$ relative to the axis of the electron beam $\mathbf{e}_1$. The expressions are obtained in the framework of two-wave approximation of dynamic diffraction theory taking into account the angle between the reflecting system of parallel atomic planes of the crystal and the target surface (angle $\delta$).

In Bragg scattering geometry, the frequency range of total external absorption (extinction) of pseudo photons of coulomb field of relativistic electron in single crystal exists that was known for real X-ray photons. In this region, the incident wave vector takes on a complex value even in absence of absorption and as the result all the photons reflect. If absorption is absent the of wave vector lengths have such a view:

$$k^{(1,2)}=\omega\sqrt{1+\chi_0'}+\frac{\omega\left|\chi_{\mathbf{g}}'C^{(s)}\right|}{2\varepsilon}\left(\xi^{(s)}(\omega)\pm\sqrt{\xi^{(s)}(\omega)^2-\varepsilon}\right). \tag{13}$$

The region of total reflection defines by following inequality:

$$-\sqrt{\varepsilon}<\xi^{(s)}(\omega)<\sqrt{\varepsilon},\ -\sqrt{\varepsilon}-\frac{1+\varepsilon}{2\nu^{(s)}}<\eta^{(s)}(\omega)<\sqrt{\varepsilon}-\frac{1+\varepsilon}{2\nu^{(s)}}, \tag{14}$$

from which one can see that the width of this range is defined by value of $2\sqrt{\varepsilon}$. It can be shown from (11b) that the width of region of total reflection practically coincides with the of DTR spectrum width.

The magnitude and the width of angular density of PXR produced by relativistic electron with energy exceeding several hundred MeV practically do not depend on the electron energy. In this connection angular density of PXR turn out insensitive to divergence of electron beam therefore we

will consider the contribution in coherent radiation of relativistic electron by DTR only.

As the result, we will obtain from (8) and (11) the expression describing the angular density of DTR in scattering geometries Laue (16) and Bragg (15):

$$\frac{dN_{\mathrm{DTR}}^{(s)}}{d\Omega}=\frac{e^2\chi_0'^2}{2\pi^2\sin^2\theta_B\left|\chi_{\mathbf{g}}'\right|C^{(s)}}\frac{\Omega^{(s)2}}{\sigma^{(s)2}\left(\left|\chi_{\mathbf{g}}'\right|C^{(s)}\sigma^{(s)}+\chi_0'\right)^2}\int\limits_{-\infty}^{\infty}\frac{\varepsilon^2}{\xi^{(s)2}+\varepsilon}\sin^2\left(b^{(s)}\frac{\sqrt{\xi^{(s)2}+\varepsilon}}{\varepsilon}\right)d\xi^{(s)}(\omega), \quad (15)$$

$$\frac{dN_{\mathrm{DTR}}^{(s)}}{d\Omega}=\frac{e^2\chi_0'^2}{2\pi^2\sin^2\theta_B\left|\chi_{\mathbf{g}}'\right|C^{(s)}}\frac{\Omega^{(s)2}}{\sigma^{(s)2}\left(\left|\chi_{\mathbf{g}}'\right|C^{(s)}\sigma^{(s)}+\chi_0'\right)^2}\varepsilon\sqrt{\varepsilon}\pi\cdot\tanh\left(\frac{b^{(s)}}{\sqrt{\varepsilon}}\right). \quad (16)$$

**4. The averaging of coherent radiation generated by a relativistic electron of the divergent beam in a crystal over angles of electron incidence.**

Let us consider the effect of the electron beam divergence on the spectral and angular characteristics of the radiation. For that, let us average radiation of an electron over all of its possible straight trajectories in the beam. As an example, we will carry out the averaging of the spectral-angular density of DTR for the electron beam with the Gauss angular distribution:

$$f(\psi)=\frac{1}{\pi\psi_0^2}\cdot\exp\left\{-\frac{\psi^2}{\psi_0^2}\right\}, \quad (17)$$

where $\psi_0$ is the divergence of the beam of radiating electrons (see figure 1-figure 2).

The magnitude and the width of angular density of PXR produced by relativistic electron with energy exceeding several hundred MeV practically do not depend on the electron energy. In this connection angular density of PXR turn out insensitive to divergence of electron beam therefore we will consider the contribution in coherent radiation of relativistic electron by DTR only. By averaging the expressions (7), (8) and (15), (16) we obtain

$$\left\langle\omega\frac{d^2N_{\mathrm{DTR}}^{(s)}}{d\omega d\Omega}\right\rangle=\frac{1}{\pi\psi_0{}^2}\int\int d\psi_\perp d\psi_{//}\exp\left\{-\frac{\psi_\perp{}^2+\psi_{//}{}^2}{\psi_0{}^2}\right\}\omega\frac{d^2N_{\mathrm{DTR}}^{(s)}}{d\omega d\Omega}, \quad (18a)$$

$$\left\langle\frac{dN_{\mathrm{DTR}}^{(s)}}{d\Omega}\right\rangle=\frac{1}{\pi\psi_0{}^2}\int\int d\psi_\perp d\psi_{//}\exp\left\{-\frac{\psi_\perp{}^2+\psi_{//}{}^2}{\psi_0{}^2}\right\}\frac{dN_{\mathrm{DTR}}^{(s)}}{d\Omega}. \quad (18b)$$

The calculation have been made for W(110) single crystal plate of thickness $L=1\,\mu\mathrm{m}$, Bragg angle $\theta_B\approx 20.5^o$, electron energy $E=10$ GeV for photons with $\sigma$ - polarization. In figure 3–figure 4 the curves are plotted by formulas (7), (8) and (18a) demonstrate the dependence of DTR spectral-angular densities on initial divergence of electron beam in Bragg and Laue scattering geometries under the fixed observation angle $\boldsymbol{\theta}$. The curves are plotted for the case of symmetric in relation to the target surface reflection of the radiation ($\varepsilon=1$). One can see in figure 3 that in Bragg scattering geometry the spectrum is wider than in Laue geometry. The DTR spectrum width practically coincides with the width of spectral range of total external reflection of radiation and does not depend on the initial beam divergence $\psi_0$ as it is seen in figure 3. Because of these facts the angular density of DTR in Bragg geometry turns out bigger than in Laue geometry, as it is seen in figure 5 and figure 6. If the asymmetry parameter $\varepsilon$ increases, then the range of total absorption, as well as the width of DTR spectrum increase (figure 7) too and as the result an increase will be observed in angular density of DTR (figure 8). So, DTR of the beam of relativistic electrons in Bragg scattering geometry can be more intensive than in Laue geometry. It is necessary to note that the values of spectral-angular and angular density of DTR strongly depend on initial divergence of the electron beam.

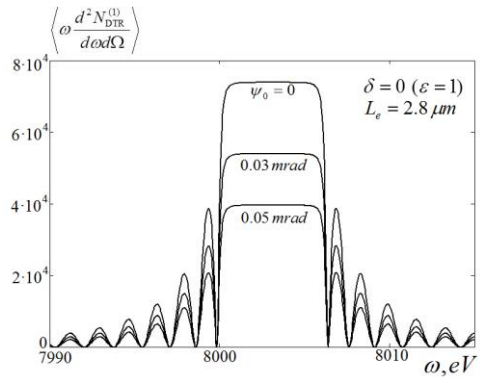


**Figure 3.** DTR spectra in Bragg scattering geometry in the range of angular density maximum under different values of electron beam divergence $\psi_0$. Symmetric reflection case ($\delta = 0$), $\theta_\perp = 0.05$ mrad, $\theta_{//} = 0$.

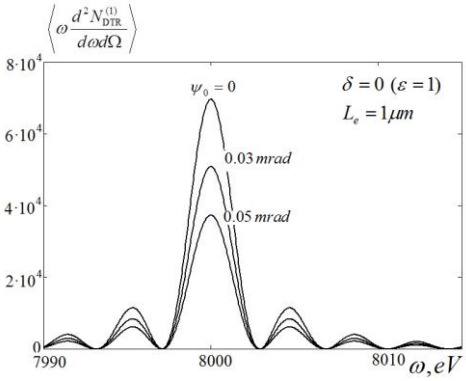


**Figure 4.** DTR spectra in Laue scattering geometry in the range of angular density maximum for different values of electron beam divergence $\psi_0$. Symmetric reflection case ($\delta = 90^o$), $\theta_\perp = 0.05$ mrad, $\theta_{//} = 0$.

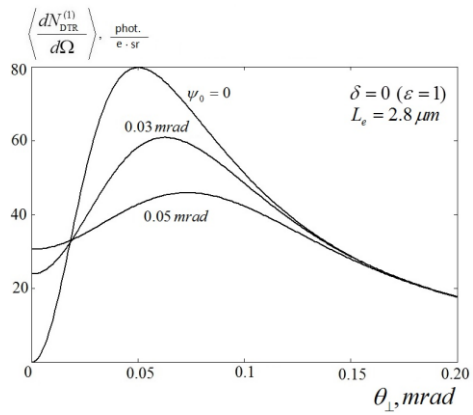


**Figure 5.** DTR angular density in Bragg scattering geometry under different values of electron beam divergence.

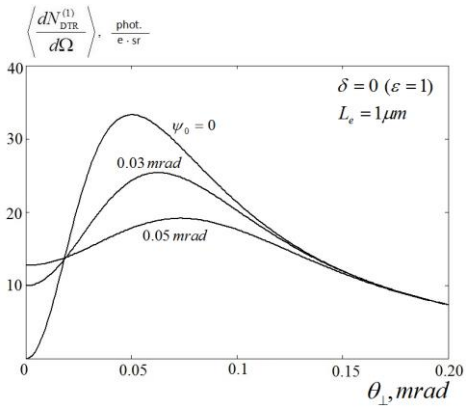


**Figure 6.** DTR spectra in Laue scattering geometry in the range of angular density maximum for different values of electron beam divergence $\psi_0$.

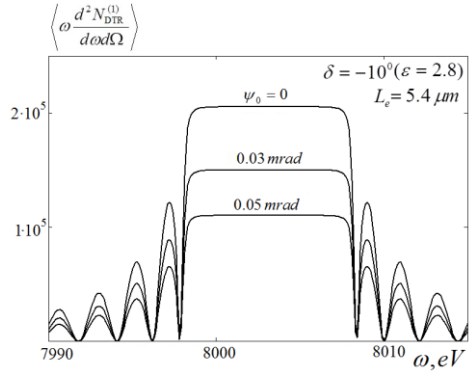


**Figure 7.** DTR spectra in Bragg scattering geometry in range of angular density maximum for different values of electron beam divergence $\psi_0$. Asymmetric reflection case ($\delta \neq 0$).

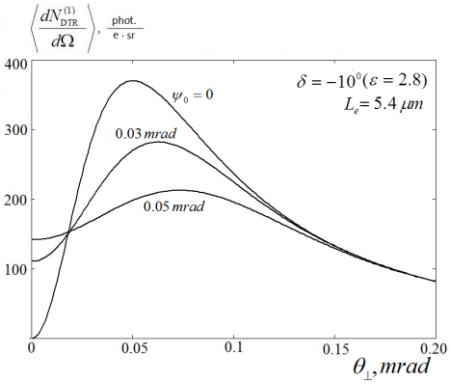


**Figure 8.** DTR angular density in Bragg scattering geometry in range of angular density maximum for different values of electron beam divergence $\psi_0$. Asymmetric reflection case ($\delta \neq 0$).

## 5. Conclusion

In the present work, the dynamic theory of coherent X-ray radiation of divergent beam of the relativistic electrons crossing a single crystal plate is considered. We have obtained the expressions for spectral-angular density parametric X-ray radiation and diffracted transition radiation of relativistic electron taking into account the deviation of electron velocity direction relative to the electron beam axis. In the framework of two-wave approximation of diffraction theory the expression for PXR and DTR are obtained for general case of asymmetric reflection of pseudo photons of the electron coulomb field. The expressions have been derived both for Laue and for Bragg scattering geometries. Based on the obtained expression for spectral-angular and angular density of the radiation of an electron in the beam using averaging over the distribution of the electron incidence angles the expressions for radiation of the electron beam as a whole have been obtained. The effect of the electron beam divergence on the angular characteristics of PXR and DTR was investigated for both cases of scattering geometry.

As an example, in the present work we carried out the averaging of the spectral-angular density of PXR and DTR for the electron beam having the Gauss angular distribution function. There was shown considerable depend of spectral-angular characteristic of DTR on divergence of electron beam. It was shown that in Bragg geometry the generation of DTR is more effective than in Laue Geometry and in condition of asymmetric reflection, the intensity of DTR can be increased additionally.

**Acknowledgements**

The Russian Science Foundation (project № 15-12-10019) supported this work.

**References**

[1] Takabayashi Y 2012 *Phys. Lett.* A **376** 2408
[2] Takabayashi Y, Sumitani K 2013 *Phys. Lett.* A **377** 2577
[3] Gogolev A, Potylitsyn A, Kube *G* 2011 *J. Phys. Conference Series* **357** 012018
[4] Sukhikh L G, Gogolev S Yu, and Potylitsyn A P 2010 *J. Phys. Conference Series* **236** 012011
[5] Konkov A S, Karataev P V, Potylitsyn A P and Gogolev A S 2014 *J. Phys. Conference Series* **517** 012003
[6] Ter-Mikaelian M 1972 *High-Energy Electromagnetic Process in Condensed Media* (New York: Wiley)
[7] Garibian G M, Yang C 1971 *J. Exp. Theor. Phys.* **61** 930
[8] Baryshevsky V G, Feranchuk I D 1971 *J. Exp. Theor. Phys.* **61** 944
[9] Ginzburg V L and Frank I M 1946 *J. Exp. Theor. Phys.* **15** 15
[10] Ginzburg V L and Tsytovich V N 1984 *Transition Radiation and Transition Scattering* (Nauka, Moscow, 1984; Adam Hilger, Bristol, United Kingdom, 1990)
[11] Caticha A 1989 *Phys. Rev.* A **40** 4322
[12] Baryshevsky V 1997 *Nucl. Instr. and Meth.* A **122** 13
[13] Artru X, Rullhusen P 1998 Nucl. *Instr. and Meth.* B **145** 1
[14] Nasonov N 1998 *Phys. Lett.* A **246** 148
[15] Blazhevich S V, Noskov A V 2008 *Nucl. Instr. and Meth.* B **266** 3770
[16] Blazhevich S, Noskov A 2009 *J. Exp. Theor. Phys.* **109** 901
[17] Blazhevich S V, Boltenko Yu A, Koskova T V, Mazilov A.A., Noskov A V 2015 *Problems of Atomic Science and Technology* **№5 (99)** 3
[18] Blazhevich S V, Koskova T V, Noskov A V 2015, *Russian Physics Journal* **58 No. 5** 585
[19] Bazylev V, Zhevago N 1987 *Emission From Fast Particles Moving in a Medium and External Fields* Moscow Nauka
[20] Blazhevich S, Noskov A 2008 *Nucl. Instr. Meth. In Phys. Res.* B **266** 3770
[21] Blazhevich S, Noskov A 2010 *J. Phys.: Conf. Ser.* **236** 012013
[22] Blazhevich S, Noskov A 2010 *J. Technical Physics* **55** 317–325